



## Control Theory

*Dennis Hens* (r0852264)  
*Nick Hosewol* (r0849415)

# Assignment 3: State Feedback and State Estimation

REPORT

Academic year 2023-2024

# Contents

<b>List of Figures</b>	ii
<b>1 Definition of a state space model and state space controller</b>	<b>1</b>
<b>2 Properties of the state estimator: a Kalman filter</b>	<b>3</b>
<b>3 Implementation of a state estimator and a state feedback controller</b>	<b>5</b>
3.1 Choice of $K$ , $Q$ and $R$ . . . . .	5
3.2 Experimental determination of $K$ . . . . .	7
3.3 Experimental analysis of $Q$ and $R$ . . . . .	7
3.4 Consistency of the Kalman filter based on the NIS and the SNIS . . . . .	8
3.5 Analysis with wrong initial estimation for the position . . . . .	10

## List of Figures

1	Schematic representation of the cart . . . . .	1
2	State space model of the system . . . . .	1
3	Position of the pole as a function of the loop gain K . . . . .	2
4	Difference between $L_\infty$ and the LQE value for L using dlqr for various values of Q and R . . . . .	5
5	Step responses and corresponding control signals for different values of K . . . . .	7
6	The evolution of $\hat{P}_{k k}$ and $L_k$ in time for different values of $\frac{Q}{R}$ after applying a step-input . . . . .	8
7	Evolution of the NIS and SNIS in time for different values of $\frac{Q}{R}$ . . . . .	9
8	Comparison between measured NIS and SNIS values and the theoretical $\chi^2$ -distribution . . . . .	10
9	Measured and estimated distance in time for different values of $\frac{Q}{R}$ . . . . .	11
10	Measured and estimated distance in time for a slow state estimator . . . . .	12

# 1 Definition of a state space model and state space controller

To design a state space estimator and controller, first, the relevant states and the relevant physical equations have to be defined. As the cart is driving in one dimension, the most obvious choice for a relevant state of our model, is the position relative to a wall. The input for the system is taken to be the rotational velocity,  $\omega$ , of the wheels of the cart (assumed to be the same for both wheels, such that the cart drives in a straight line). This velocity is assumed to be exactly equal to the 'desired velocity' the state feedback controller determines. (This assumption boils down to the assumption that the PI controller designed in the last report works perfectly and immediately.) The state is measured using an infrared sensor in the front of the cart, with a working range from 5 cm up to 30 cm.

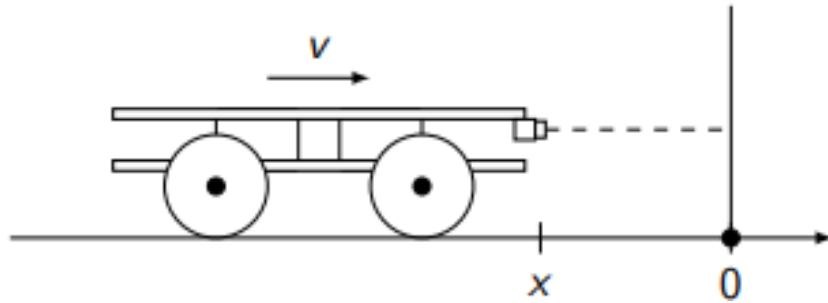


Figure 1: Schematic representation of the cart

Figure 1 shows a schematic of the cart and its state. Because the position sensor is in front of the cart, the absolute coordinate of the position of the cart is negative. The origin of the reference frame is chosen on the detected wall. Due to the fact that the sensor measures absolute distance, the sensor returns the value  $-x$  in a measurement.

$$\frac{dx}{dt} = v = \omega \cdot \frac{D}{2} \quad (1)$$

Equation 1 shows the relevant kinematic laws describing the motion of the cart.  $D$  is the diameter of the wheels, and equals 0.065 m. Discretising this equation using the forward Euler method yields equation 2.

$$\begin{aligned} \frac{dx}{dt} &= \omega \cdot \frac{D}{2} \\ \Leftrightarrow \frac{x[k+1] - x[k]}{T_s} &= \omega \cdot \frac{D}{2} \\ \Leftrightarrow x[k+1] &= x[k] + T_s \cdot \omega \cdot \frac{D}{2} \end{aligned} \quad (2)$$

The state space model for this example is shown below.

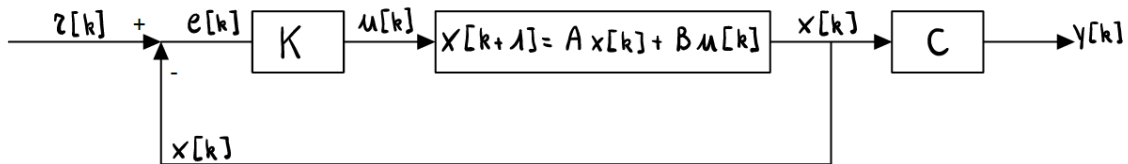


Figure 2: State space model of the system

Figure 2 shows the state space model, which is characterised by the matrices  $A$ ,  $B$ ,  $C$ . Since the system is strictly proper, the usual matrix  $D$  is not included in the drawing, nor the system. In this discrete time model, the state space matrices are given by  $A = 1$  and  $B = T_s \cdot \frac{D}{2}$ , as derived in equation 2. Because this model only has one state, these matrices simplify to be scalar numbers. The input of the model is a reference signal  $r[k]$ , which the cart (or in this case, the state of the cart system) will be supposed to follow.

The transfer function of the closed loop system can be derived very easily. Equation 3 shows this derivation based on the error term  $e[k]$ . The assumption of scalar numbers is immediately implemented here.

$$\begin{aligned}
& \begin{cases} E(z) &= R(z) - X(z) \\ zX(z) &= AX(z) + BU(z) \\ U(z) &= KE(z) \\ C^{-1}Y(z) &= X(z) \end{cases} \\
& \iff \begin{cases} E(z) &= R(z) - C^{-1}Y(z) \\ zC^{-1}Y(z) &= AC^{-1}Y(z) + BKE(z) \end{cases} \\
& \iff (z - A + BK)C^{-1}Y(z) = BKR(z) \\
& \iff \frac{Y(z)}{R(z)} = \frac{CBK}{z - A + BK}
\end{aligned} \tag{3}$$

The pole,  $p$ , of the system is therefore given by  $p = A - BK$ , where  $A$  and  $B$  are the earlier defined matrices, and  $K$  is the control loop gain. For this pole to be stable, its magnitude has to be smaller than 1. Equation 4 shows how this limits the acceptable values of  $K$ .

$$\begin{aligned}
& -1 < p < 1 \\
& \iff -1 < A - BK < 1 \\
& \iff \frac{1 + A}{B} > K > \frac{A - 1}{B} \\
& \iff \frac{4}{T_s D} > K > 0 \\
& \iff 6153.8 > K > 0
\end{aligned} \tag{4}$$

Figure 3 shows how this pole evolves for varying positive values of  $K$ .

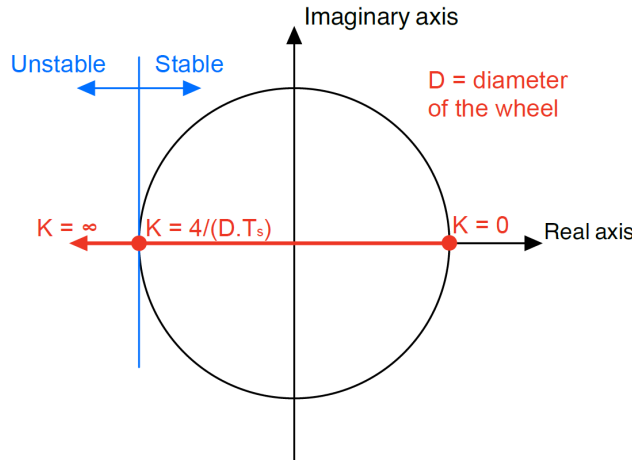


Figure 3: Position of the pole as a function of the loop gain  $K$

As figure 3 shows, the closed loop gain cannot be chosen larger than  $K = \frac{4}{D \cdot T_s}$ , because this would lead to a pole outside the unit circle, and thus create instability. This is to be understood intuitively as follows: If  $K > \frac{4}{D \cdot T_s}$ , then for a certain error  $e[k] = 1$  at time step  $k$ , the applied rotational velocity would be  $\omega > \frac{4}{D \cdot T_s} \implies v > \frac{2}{T_s}$ . This velocity is at least kept until step  $k + 1$ , which takes a time  $t = T_s$ . The laws of kinematics now imply that  $e[k] < -1$  (if the reference signal stays constant, that is), therefore creating instability. A negative value for  $K$  would also lead to an unstable system. This is very intuitive: if a positive error is measured, the controller would induce a negative velocity, therefore increasing the error. If the pole is chosen towards the origin, near  $K = \frac{2}{D \cdot T_s} \approx 3077$  the response speed of the state feedback controller increases, as the pole moves towards higher frequencies. Using the explanation above, the exact value for  $K = \frac{2}{D \cdot T_s} = 3077$ , would indeed completely erase the error in one time step. For realistic values of  $K$  however (which are definitely below  $K = 1000$ , as will be elaborated on later), an increase of  $K$  means a faster response speed.

As the distance sensor measures absolute distance and the reference axis is chosen to be in front of the cart,

the measurement equation is given by  $y[k] = -x[k]$ , from which follows that  $C = -1$  and  $D = 0$ . This system is strictly proper, as the reference position does not influence the measurement.

## 2 Properties of the state estimator: a Kalman filter

A Kalman filter is an estimator that estimates the states of a given system using variable gains. In this estimator  $\vec{x}$  is the estimate of the state  $\vec{x}$ . Such a system is given by equation 5. We have assumed the system is strictly proper, as this is also the case for the cart.  $w_k$  and  $v_k$  are the process noise and measurement noise respectively, which follow a Gaussian distribution with average 0, and covariance matrix  $Q_k$  and variance  $R_k$ . The process noise of the system refers to the error made in the state equation, for example by assumptions or approximations made in said equations. The measurement noise, on the other hand, is fully determined by the uncertainty that the distance sensor introduces.

$$\begin{cases} \vec{x}_{k+1} &= A\vec{x}_k + Bu_k + \vec{w}_k \\ y_k &= C\vec{x}_k + v_k \end{cases} \quad (5)$$

$P_{k|k}$  is the a posteriori covariance matrix of the state error,  $x - \hat{x}$ , which is estimated with  $\hat{P}_{k|k}$  at time instance  $k$  (which refers to the first  $k$ , as is usual in statistics), if the measurement value  $y_k$  is known.

The exact mathematical workings of the Kalman filter are beyond the scope of this report, but certain important results concerning the covariance matrix  $\hat{P}_{k|k}$  and the optimal Kalman gain  $L_k$ , which determines how  $\vec{x}_{k+1|k}$  and  $y_{k+1}$  are combined to form a new estimate,  $\vec{x}_{k+1|k+1}$ , are calculated here. The formulas used, come from C9 in *Control Theory* [1]. Note that in a Kalman filter, this value is time dependant, in contrast with a linear quadratic estimator, for example.

Equation 6 calculates the optimal Kalman gain for the next time step  $k + 1$  as a function of  $\hat{P}_{k|k}$ ,  $Q$  and  $R$ , of which  $Q$  and  $R$  are assumed to be independant of  $k$ . Due to the fact that our cart system only admits one state, all earlier defined matrices and vectors reduce to scalar values (likewise, the state space matrices also reduced to scalars in section 1). Remember that  $A = 1$ ,  $B = \frac{T_s D}{2}$  and  $C = -1$ .

$$\begin{aligned} L_{k+1} &= \hat{P}_{k+1|k} C S_{k+1}^{-1} \\ L_{k+1} &= (A^2 \hat{P}_{k|k} + Q) C (C^2 (A^2 \hat{P}_{k|k} + Q) + R)^{-1} \\ L_{k+1} &= \frac{C(A^2 \hat{P}_{k|k} + Q)}{C^2 (A^2 \hat{P}_{k|k} + Q) + R} \\ L_{k+1} &= \frac{-(\hat{P}_{k|k} + Q)}{\hat{P}_{k|k} + Q + R} \end{aligned} \quad (6)$$

Here,  $S_{k+1}$  is the covariance of the residual,  $\nu_{k+1} = y_{k+1} - C\hat{x}_{k+1|k}$ . Equation 7 shows the limit cases as the variances  $Q$  and  $R$  grow large.

$$\begin{aligned} \lim_{Q \rightarrow \infty} (L_{k+1}) &= \lim_{Q \rightarrow \infty} \left( \frac{-Q}{Q} \right) = -1 \\ \lim_{R \rightarrow \infty} (L_{k+1}) &= \lim_{R \rightarrow \infty} \left( \frac{-(\hat{P}_{k|k} + Q)}{R} \right) = 0 \end{aligned} \quad (7)$$

These results are very logical. If, for instance, the measurement noise variance,  $R$ , is infinite, your measurement is completely arbitrary, resulting in useless measurements. If the measurement contains no useful information on the state,  $x$ , it should be omitted from the correction step, therefore  $L = 0$ . If, on the other hand, the process noise covariance is infinite, we should fully rely on the measurements. A value of  $L_{k+1} = -1$  leads to equation 8 for  $x_{k+1|k+1}$ .

$$\begin{aligned} \hat{x}_{k+1|k+1} &= \hat{x}_{k+1|k} - 1 \cdot (y_{k+1} - C\hat{x}_{k+1|k}) \\ \hat{x}_{k+1|k+1} &= -y_{k+1} = Cy_{k+1} \end{aligned} \quad (8)$$

This short calculations explains intuitively why the value of  $L = -1$  is optimal: The initial guess for the state  $x_{k+1|k}$  is completely disregarded, and replaced with the measurement. (Which is logical, as for  $Q \rightarrow \infty$ , the initial guess before the correction step is completely useless.)

Equation 9 shows how the variance of the state estimate,  $\hat{P}_{k|k}$  evolves for every time step, after the measurement is known.

$$\begin{aligned}
& \hat{P}_{k+1|k+1} = \hat{P}_{k+1|k} - \hat{P}_{k+1|k}^2 C^2 (S_{k+1}^{-1}) \\
\iff & \hat{P}_{k+1|k+1} = \hat{P}_{k+1|k} \left(1 - \frac{\hat{P}_{k+1|k}}{\hat{P}_{k+1|k} + R}\right) \\
\iff & \hat{P}_{k+1|k+1} = \hat{P}_{k+1|k} \frac{C^2 R}{C^2 \hat{P}_{k+1|k} + R} \\
\iff & \hat{P}_{k+1|k+1} = \frac{(\hat{P}_{k|k} + Q)R}{\hat{P}_{k|k} + Q + R}
\end{aligned} \tag{9}$$

The limit of this value in the extreme cases for  $Q$  and  $R$  is given by equation 10.

$$\begin{aligned}
\lim_{Q \rightarrow \infty} (\hat{P}_{k|k}) &= \lim_{Q \rightarrow \infty} \left( \frac{QR}{Q} \right) = R \\
\lim_{R \rightarrow \infty} (\hat{P}_{k|k}) &= \lim_{R \rightarrow \infty} \left( \frac{(\hat{P}_{k|k} + Q)R}{R} \right) = \hat{P}_{k|k} + Q
\end{aligned} \tag{10}$$

These limits are very logical: if the variance of the process noise,  $Q$  is infinitely large, our state estimate before measurement,  $x_{k+1|k}$ , is completely unreliable, and the a posteriori state estimate is equal to the measurement, as proven in equation 8. In this case, the new variance would be equal to the variance in the measurement error,  $R$ . On the other hand, if the variance of the measurement error,  $R$ , is infinitely large, the measurement does not contribute to the estimation process, as was shown in equation 7. Therefore, the new variance of the state estimate is the sum of the variance of the previous estimate and the variance of the process noise, as this estimate uses the the state equations, which introduces the process noise  $Q$ .

By taking the limit as  $k$  approaches infinity of the recurrence relation defined in equation 9, the steady state variance of the state estimate is calculated, as shown in equation 11

$$\begin{aligned}
& \hat{P}_\infty = \frac{(\hat{P}_\infty + Q)R}{\hat{P}_\infty + Q + R} \\
\iff & \hat{P}_\infty (\hat{P}_\infty + Q + R) = (\hat{P}_\infty + Q)R \\
\iff & \hat{P}_\infty^2 + Q\hat{P}_\infty - QR = 0 \\
\iff & \hat{P}_\infty = \frac{-Q \mp \sqrt{Q^2 + 4QR}}{2} \\
\iff & \hat{P}_\infty = \frac{-Q + \sqrt{Q^2 + 4QR}}{2}
\end{aligned} \tag{11}$$

Obviously, only the positive solution is valid, as  $\hat{P}_\infty$  has to be a positive value. From this, the steady state Kalman gain is calculated in equation 12.

$$\begin{aligned}
& L_\infty = \frac{-(\hat{P}_\infty + Q)}{\hat{P}_\infty + Q + R} \\
\iff & L_\infty = \frac{-(-Q + \sqrt{Q^2 + 4QR} + 2Q)}{-Q + \sqrt{Q^2 + 4QR} + 2Q + 2R} \\
\iff & L_\infty = \frac{-Q - \sqrt{Q^2 + 4QR}}{Q + \sqrt{Q^2 + 4QR} + 2R}
\end{aligned} \tag{12}$$

For a constant noise ratio, which is assumed, the steady state Kalman gain should converge towards the optimal Linear Quadratic Estimator (LQE) gain, which can be calculated numerically, using the state parameters and the command *dlqr* in *MATLAB*. As shown in figure 4, the difference between the theoretical steady state Kalman gain,  $L_\infty$  and the LQE-value, denoted  $L$  in the figure, is down to machine precision for different values of  $Q$  and  $R$ , therefore solidifying this theoretical value for the steady state Kalman gain as correct.

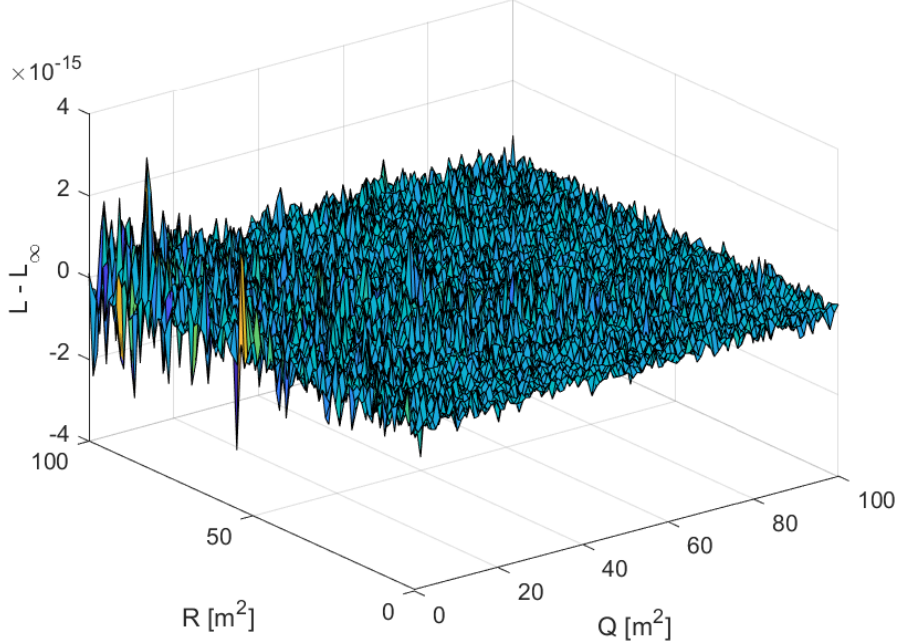


Figure 4: Difference between  $L_\infty$  and the LQE value for L using dlqr for various values of  $Q$  and  $R$

For an LQE, the closed loop pole,  $p$ , is given by equation 13. Using the expression for the steady state Kalman gain, which should equal the optimal LQE gain, the pole is written as a function of  $\frac{Q}{R}$ .

$$\begin{aligned}
 p &= A(1 - LC) \\
 \iff p &= 1 + L_\infty \\
 \iff p &= 1 + \frac{-Q - \sqrt{Q^2 + 4QR}}{Q + \sqrt{Q^2 + 4QR} + 2R} \\
 \iff p &= \frac{2R}{Q + \sqrt{Q^2 + 4QR} + 2R} \\
 \iff p &= \frac{2}{\frac{Q}{R} + \sqrt{\left(\frac{Q}{R}\right)^2 + 4\frac{Q}{R}} + 2}
 \end{aligned} \tag{13}$$

For  $\frac{Q}{R} = 0$ , this pole lies on the unit circle at  $p = 1$ . For increasing  $\frac{Q}{R}$ , this pole moves towards the origin, with a pole at  $p = 0$  for  $\frac{Q}{R} \rightarrow \infty$ . Therefore, it is not possible to make the system unstable by varying  $\frac{Q}{R}$ , unless  $Q$  is uniquely zero. As this ratio grows larger, the LQE system should converge faster, as the pole moves towards higher frequencies. As the Kalman filter does not have time-independent poles, this train of thought cannot be extended entirely. However, as the Kalman filter is designed to have an optimal state covariance  $\hat{P}_{k|k}$  at every time step, it converges faster, such that the same trend occurs: a higher  $\frac{Q}{R}$  ratio increases the speed of the Kalman filter. If the chosen value for the ratio is chosen way higher than the actual ratio the physical system has, the Kalman filter starts accurately tracking the noise, which loses the smoothness the state estimator should exhibit. It is therefore wise to accurately choose the trade-off between the convergence speed and following noise.

### 3 Implementation of a state estimator and a state feedback controller

#### 3.1 Choice of $K$ , $Q$ and $R$

To accurately choose the values for the process and measurement covariances  $Q$  and  $R$ , the sources of these noise have to be identified. First of all, The infrared sensor's intrinsic uncertainty poses a source of measurement noise. Various external factors, including ambient light, dust, and vibrations could contribute to this

noise encountered by the infrared sensor. Additionally, the infrared sensor's range limitation serves as another contributor to measurement noise. The sensor's operational range is confined to  $5 - 30\text{ cm}$ . Should the cart be positioned closer than  $5\text{ cm}$  or exceed the distance of  $30\text{ cm}$  from the wall, the sensor's capacity to deliver precise distance measurements is compromised.

The process noise is harder to exactly determine, but there are a few contributing factors. Even though the kinematic equation  $v = \frac{dx}{dt}$  is exactly correct, the assumption that the velocity of the cart is exactly the desired velocity  $v$  is an approximation, dependant on the quality of the velocity controller. Furthermore, if the wheel slips during operation (which is actually a requirement to build up the frictional force pushing the cart), the relation  $v = \omega \cdot \frac{D}{2}$  is also an approximation.

Choosing appropriate values for the control gain  $K$ , the process noise covariance  $Q$ , the measurement noise covariance  $R$ , and the initial state covariance matrix  $\hat{P}_{0|0}$  requires careful consideration of various trade-offs to achieve optimal performance of the Kalman filter. The control gain  $K$  determines the responsiveness and stability of the system. Higher values of  $K$  can result in a faster response, but they also increase the risk of overshooting or instability. Therefore, finding a right balance between performance requirements and stability is important to choose a good value for  $K$ . The initial state covariance matrix  $\hat{P}_{0|0}$  determines the confidence in the initial state estimate. If  $\hat{P}_{0|0}$  is chosen to be very small, the initial state estimate is very close to the actual value of the state of the system. In the Kalman filter, this value ( $\hat{P}_{k|k}$ ) is updated along with the state estimate for every time step, showing the uncertainty of the state in time. If  $\hat{P}_{0|0}$  is relatively large, the Kalman filter will converge quickly to the measurements.

The value of  $R$  can be easily derived through an experimental setup. To determine the value of  $R$ , the distance sensor is put at the middle point of its range, at  $18\text{ cm}$ , and does not move for a certain time. Due to the uncertainty in the measurement of the sensor, this perfectly measures the noise around the average measurement of  $18\text{ cm}$ . By loading the measurements into *MATLAB* and calculating the variance of this data sets, the measurement variance  $R$  is determined to be  $R = 5.5990 \cdot 10^{-6}\text{ m}^2$ . Note that the variance changes as a function of the average distance. This could lead to added inaccuracies.

As will be discussed later, to set up most experiments, the carts measurement sensor is activated, and the cart is positioned manually, such that the measurements average out to be the desired starting position. By doing this, the initial covariance matrix  $\hat{P}_{0|0}$  can be approximated by the variance on the measurement sensor, such that  $\hat{P}_{0|0} = 5.5990 \cdot 10^{-6}\text{ m}^2$ . If this value is very low, the Kalman filter will trust the initial guess more. If this value would be very high, however, the Kalman filter will immediately update the state to the first measurement and proceed from there.

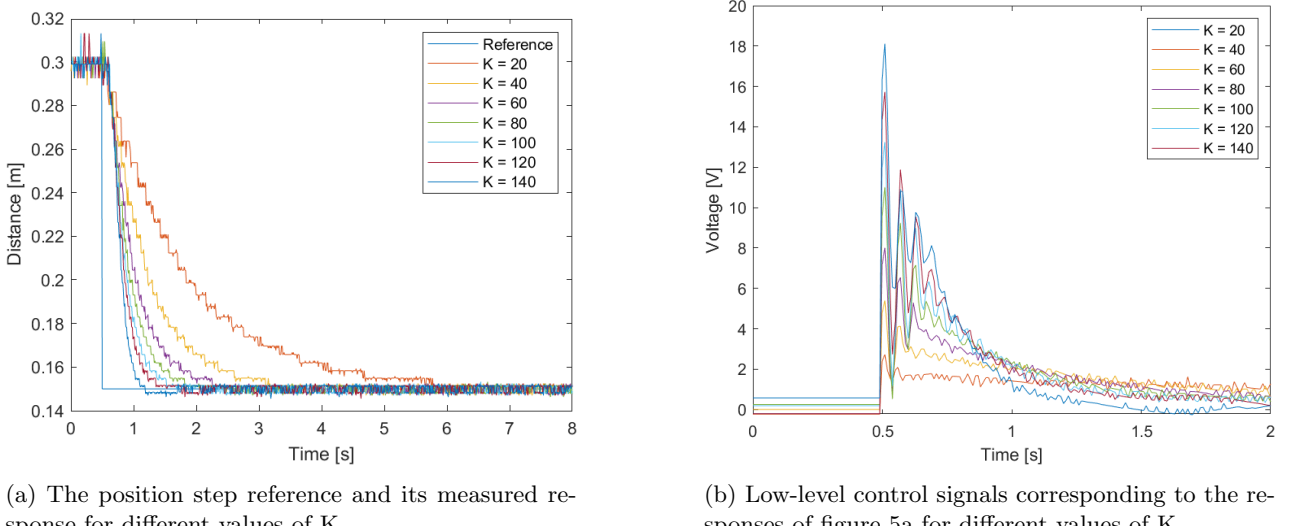
An exact value for the process noise variance  $Q$  and the optimal value for the feedback gain  $K$  are harder to obtain, and have to be determined using practical experiments. The former could be determined experimentally by using the *NIS* and *SNIS* consistency tests for several values of  $\frac{Q}{R}$  and checking which  $Q$ -value grants the results which are best in line with the expected statistical distribution. This will further be discussed later. For the rest of the assignment, the value for  $Q$  will be taken to be  $10^{-7}\text{ m}^2$ , as this led to good results in the experiments determining the value for  $K$ . In particular, the cart did not behave 'nervous', which means the cart keeps oscillating very quickly due to it trying to follow the measurement noise, but, on the other hand, the estimator also tracked the actual state very well. (Which implies the estimator is not 'overconfident' in its state model, leading to disregarding the measurements.) This value leads to a  $\frac{Q}{R}$  ratio equal to 0.018. Note that even though  $Q$  has an actual physically correct value, a Kalman filter (mis)treats this as a design parameter. If, for instance, a Kalman filter on a chemical plant is just supposed to converge as quickly as physically possible, without caring about the filter following measurement noise, then  $Q$  should be chosen really low, even if in physical reality the  $Q$ -value is really high. The value for  $K$  will be determined in section 3.2, using experimental evidence. As the distance the cart has to drive (which is the initial difference between the state and the reference) is on the order of  $10^{-2}\text{ m}$  and the realistic range of desired velocities (velocities the controller will (try to) impose) is maximally approximately equal to  $\omega = 20 \frac{\text{rad}}{\text{s}}$ , such that values around  $K = 200$  and lower are feasible. As the actual initial reference error in section 3.2 is chosen to be  $15 \cdot 10^{-2}\text{ m}$  and some safety margin in the velocity of the wheels is desirable, the range of  $K$  is chosen to be from 20 to 140. After some other experiments with varying  $Q$  and  $K$  the chosen values are listed in table 1.

Variable	Value	Unit
$K$	100	$\frac{rad}{s \cdot m}$
$Q$	$10^{-7}$	$m^2$
$R$	$5.5990 \cdot 10^{-6}$	$m^2$
$\hat{P}_{0 0}$	$5.5990 \cdot 10^{-6}$	$m^2$

Table 1: Chosen values for  $K$ ,  $Q$ ,  $R$  and  $\hat{P}_{0|0}$

### 3.2 Experimental determination of $K$

Now a step signal as position reference is applied to the cart. The cart starts on 30 cm and after some time the desired distance from the wall is set to 15 cm. The distance from the wall is given by using the sensor measurements directly. The initial state estimate was chosen to be correct at  $\hat{x}_{0|0} = -30$  cm. The step reference together with the measured response is plotted in figure 5a for different values of  $K$ . In figure 5b the low-level control signals (voltages) corresponding to the responses of figure 5a are plotted for different values of  $K$ . As seen in this figure, the higher the value of  $K$ , the higher the desired voltage applied to the cart is. This would lead, for the values plotted, to a quicker displacement towards the reference distance, as a higher applied voltage is directly the result of a higher desired velocity, and thus to a faster convergence. Because the maximum applicable voltage to the motors is 12 V,  $K$  is constrained to prevent the requested control signal from demanding a voltage greater than 12 V, as a higher value for  $K$  would not have any benefits. For this reason,  $K$  is chosen to be 100  $\frac{rad}{s \cdot m}$ . As discussed earlier, the practical range of  $K$  values does not come close to values which induce instability. More even, the practical values for  $K$  are limited to the range where an increasing  $K$  always leads to a faster controller. The limit for  $K$  is therefore rather practical than theoretical.



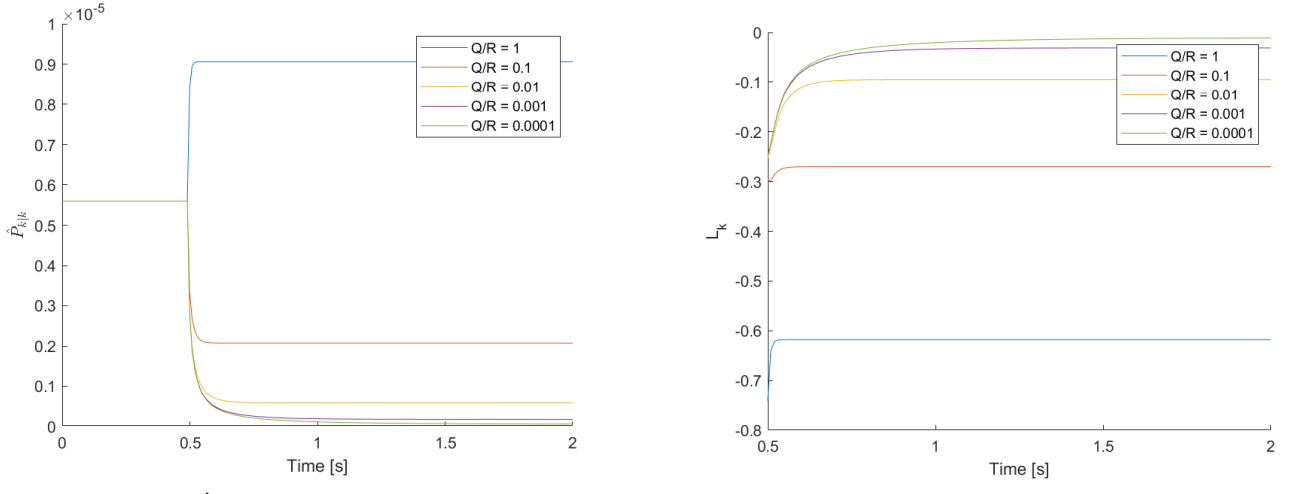
(a) The position step reference and its measured response for different values of  $K$

(b) Low-level control signals corresponding to the responses of figure 5a for different values of  $K$

Figure 5: Step responses and corresponding control signals for different values of  $K$

### 3.3 Experimental analysis of $Q$ and $R$

Next the same step signal as before is applied to the cart but now for different values of  $Q$  and  $R$ . Because we determined the value of  $R$  experimentally with a certain degree of confidence, we will only vary  $Q$  such that the ratio  $\frac{Q}{R}$  still varies. The evolution of  $\hat{P}_{k|k}$  and  $L_k$  in time are plotted in figure 6 for different ratios of  $\frac{Q}{R}$ . As seen in this figures the values of  $\hat{P}_{k|k}$  and  $L_k$  indeed converge towards  $\hat{P}_\infty$  and  $L_\infty$  respectively. If we take  $Q = 5.5990 \cdot 10^{-8} m^2$  and  $R = 5.5990 \cdot 10^{-6} m^2$  for example we get using equations 11 and 12:  $\frac{Q}{R} = 0.01$ ,  $\hat{P}_\infty = 5.3 \cdot 10^{-7} m^2$  and  $L_\infty = -0.0951 m^2$ . This corresponds to the values in figure 6. Besides the steady state values, the convergence speed of the Kalman filter is also observed to be higher for higher  $\frac{Q}{R}$  ratios. This convergence speed however, compromises the smoothness of the estimated state. These observations are completely in line with the theoretical explanation earlier.



(a) Evolution of  $\hat{P}_{k|k}$  in time after applying a step input for different values of  $\frac{Q}{R}$

(b) Evolution of  $L_k$  in time after applying a step input for different values of  $\frac{Q}{R}$

Figure 6: The evolution of  $\hat{P}_{k|k}$  and  $L_k$  in time for different values of  $\frac{Q}{R}$  after applying a step-input

### 3.4 Consistency of the Kalman filter based on the NIS and the SNIS

In what follows we will investigate whether the developed Kalman filter is inherently consistent. If there are some modelling errors in the system model or noise models, for example, the Kalman filter could estimate erroneous values that cannot be explained statistically. This leads to the principle of statistical tests which are supposed to identify the consistency of the Kalman filter. An optimal criterion would involve the exact estimation error (the *NEES* criterion), but as the exact state is not known, this section will discuss the NIS and SNIS criteria. The NIS and SNIS are given by equations 14 and 15:

$$NIS_k = \nu_k^T S_k^{-1} \nu_k \quad (14)$$

$$SNIS_k = \sum_{j=k-M+1}^k \nu_j^T S_j^{-1} \nu_j \quad (15)$$

where  $\nu_{k+1}$  and  $S_{k+1}$  are defined by equation 16

$$\begin{aligned} \nu_k &= y_k - C\hat{x}_{k|k} \\ \iff \nu_k &= y_k + \hat{x}_{k|k} \\ S_{k+1} &= C\hat{P}_{k+1|k}C^T + R_{k+1} \\ \iff S_{k+1} &= \hat{P}_{k+1|k} + R_{k+1} \end{aligned} \quad (16)$$

The innovation  $\nu$  is defined to be the error between the measurement value and the predicted measurement value, which is based to the state estimate. The innovation covariance  $S$  is the covariance of this stochastic variable. The NIS can be interpreted as the error between the measurements and the state estimates, which can be interchangeably viewed as 'approximations' of the state itself and the state estimate. As the innovation follows a Gaussian distribution, the NIS is a  $\chi^2$  distribution with the amount of degrees of freedom equal to the amount of states. As the SNIS is the sum of 5 (which is arbitrarily chosen in this assignment) NIS values, this stochastic variable is also a  $\chi^2$  distribution, with 5 degrees of freedom. To check the consistency of the Kalman filter we need to check whether these stochastic variables are actually distributed as theory predicts and to check whether the guessed values of  $Q$ ,  $R$ ,  $\hat{P}_{0|0}$  and  $\hat{x}_{0|0}$  were guessed correctly by analysing the NIS and SNIS distributions in time. This is now put into practice. The evolution of the NIS and SNIS in time are plotted in figure 7 for different values of  $\frac{Q}{R}$ . In these plots, only  $Q$  was varied, as the measurement covariance  $R$  was determined accurately in another experiment.

As figure 7 shows, the best values for the NIS and SNIS 95% are found for  $\frac{Q}{R} = 0.01$ , which corresponds to the value which was chosen earlier in the report. This 'best' score, however, is still not good enough to

strongly conclude anything about the consistency of the designed Kalman filter. Figure 7f shows a zoom of the confidence interval for the chosen  $\frac{Q}{R}$  ratio. The figure clearly shows that the data points are mostly at the bottom of the interval. This clearly indicates that, even though the  $\frac{Q}{R}$  ratio was chosen relatively well, both  $Q$  and  $R$  were chosen too large. To optimise the Kalman filter, the design process this report walked through could now be repeated with better estimates, which would in turn lead to better NIS and SNIS plots.

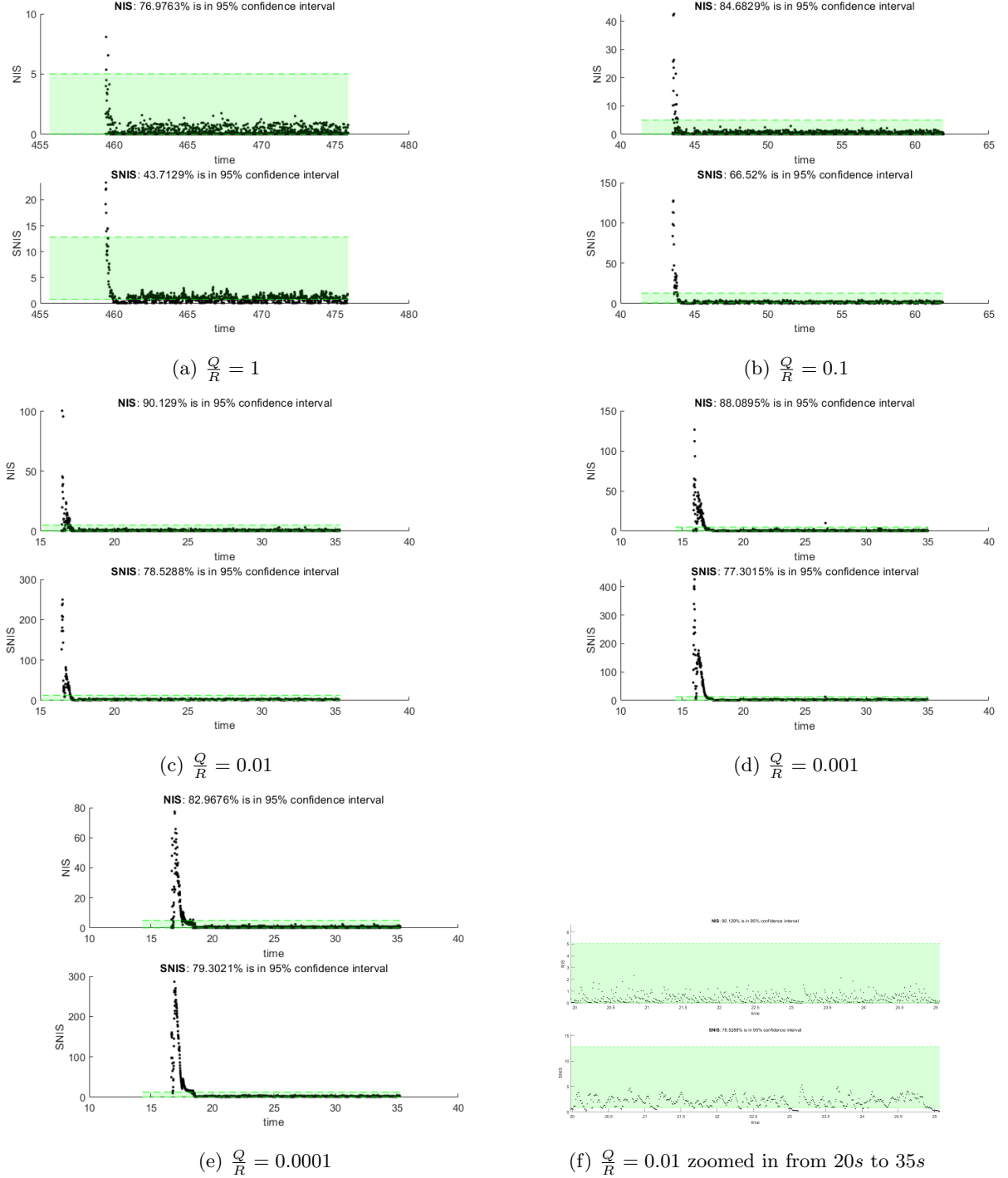


Figure 7: Evolution of the NIS and SNIS in time for different values of  $\frac{Q}{R}$

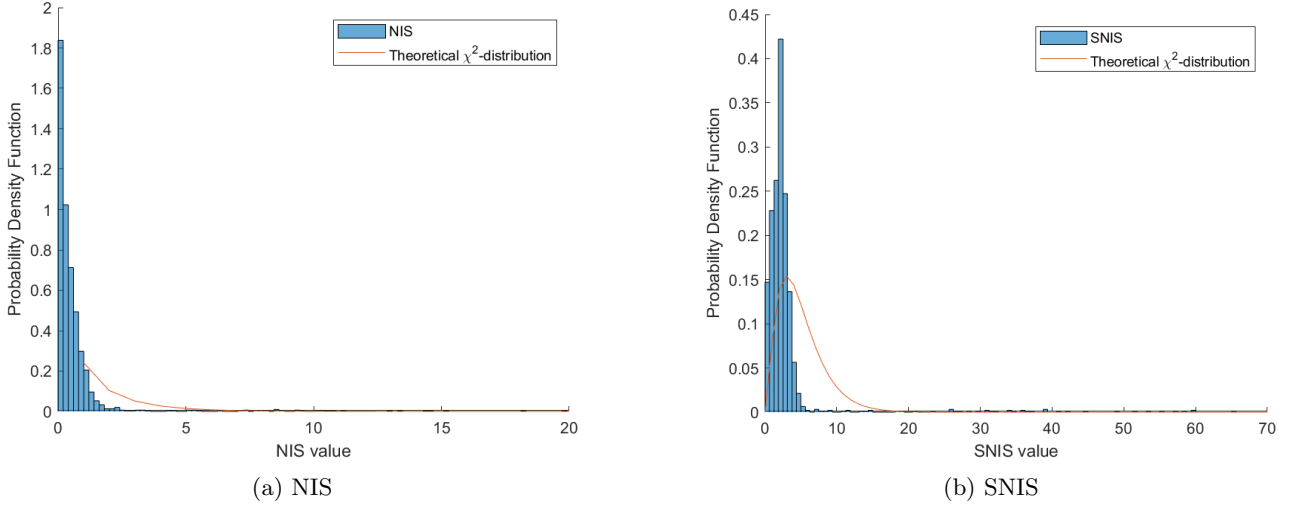


Figure 8: Comparison between measured NIS and SNIS values and the theoretical  $\chi^2$ -distribution

Figure 8 shows the probability distribution for the NIS and SNIS data acquired using a histogram. The data of figure 7c was used, as this corresponds to the Kalman filter that was implemented. The histogram clearly shows a deviation from the expected  $\chi^2$ -distribution. For the NIS distribution, the first peak could be explained by the fact that a  $\chi^2$  distribution with 1 degree of freedom does have a vertical asymptote, but the weight is still not distributed perfectly. In the SNIS plot however, it's very clear that there is a bias for the lower SNIS values. It is therefore safe to conclude that the measured NIS and SNIS are not  $\chi^2$  distributed, as they are supposed to be. The problem lies at the heart of the Kalman filter: one of the main assumptions entails that both the process noise and the measurement noise are distributed normally, which would imply the NIS and SNIS follow a  $\chi^2$  distribution. This assumption clearly does not match reality. Returning to the original question, this proves that the Kalman filter is not entirely consistent.

### 3.5 Analysis with wrong initial estimation for the position

Until this point, the initial state estimate has always been chosen as accurately as possible. This section analyses the influence of the  $\frac{Q}{R}$  ratio on the convergence speed of the state estimator, while applying the same step input as before. The cart starts on 30 cm and after some time the desired distance from the wall is set to 15 cm, but the initial position  $\hat{x}_{0|0}$  is chosen to be  $-10 \cdot 10^{-2} m$ , so 10 cm in front of the the wall. The  $R$  value is kept constant to the earlier measured value, while the  $Q$  value is altered to get the desired  $\frac{Q}{R}$  ratio. The evolution of the position estimate and the measured position by the infrared sensor in time is plotted in figure 9 for different values of  $\frac{Q}{R}$ . It can be seen in the figure that the higher the  $\frac{Q}{R}$  ratio, the faster the estimates converge to the measurements. This is logical, because a higher  $\frac{Q}{R}$  ratio means a higher value for  $Q$  for a constant value of  $R$ . A higher  $Q$  will result in less trust in the actual state estimate and more trust in the measurements (as a lower  $R$  with a constant  $Q$  would as well). This is completely in line with the earlier observations that a higher  $\frac{Q}{R}$  ratio leads to a faster convergence of the Kalman filter. Note that the trade-off is also visible here:  $\frac{Q}{R} = 1$  converges practically immediately, but the estimator follows the noise on the measurement almost exactly, which leads to a less smooth control action.

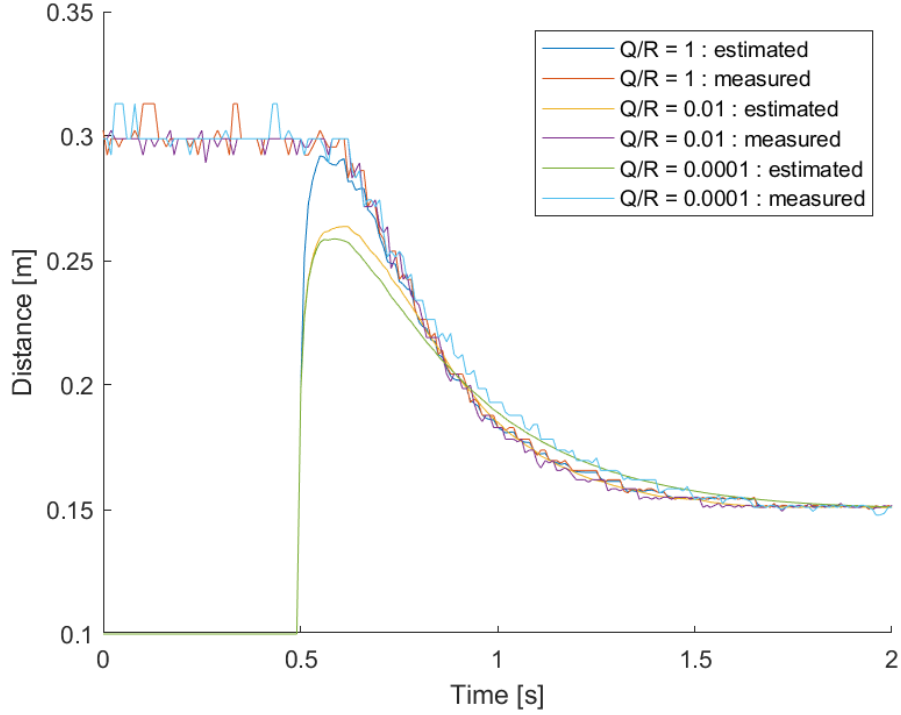


Figure 9: Measured and estimated distance in time for different values of  $\frac{Q}{R}$

To highlight the importance of the convergence speed of the estimator, a new simple prediction estimator is designed using pole placement. The state estimator will be designed such that the closed-loop pole of the estimator is 10 times slower than the closed-loop pole of the state feedback controller that was chosen. To determine the frequency of this pole, equation 3 is used to determine the frequency of the controller pole. Using the values of  $A = 1$ ,  $B = T_s \cdot \frac{D}{2} = 3.25 \cdot 10^{-4} s \cdot m$  and  $K = 100 \frac{\text{rad}}{s \cdot m}$ , the controller pole is located at  $z = 0.9675$ . Equation 17 shows the transformation formula from the discrete pole to the continuous pole.

$$p_c = \frac{\ln(p_d)}{T_s} \quad (17)$$

The controller pole is therefore located at  $p_c = 20.76 \text{ Hz}$ . A pole that's 10 times slower, is located at  $p'_c = 2.076 \text{ Hz}$ , such that  $z' = 0.997$ . Now, to determine the correct estimator gain for the prediction estimator, such that the estimator has a pole at  $z = 0.997$ , the *MATLAB* command *place* is used, together with the necessary state parameters (which are  $A^T$  and  $C^T$ ). This yields a fixed estimator gain equal to  $L = -0.003299$ . This estimator works exactly like the Kalman filter, only the correction step now uses this constant gain, to ensure the pole stays at the desired frequency. Note that the estimator pole is usually chosen 2 to 6 times faster than the control pole as a rule of thumb.

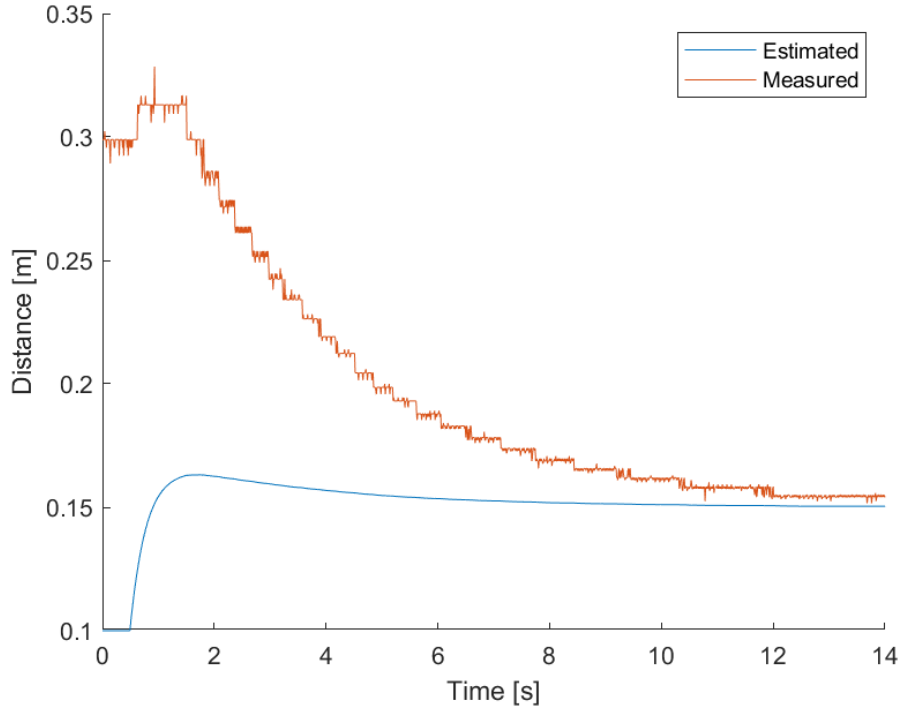


Figure 10: Measured and estimated distance in time for a slow state estimator

Now the step input used before is applied, again with the same wrong initial estimate for the position. The evolution of the measured distance together with the estimated distance in time are plotted in figure 10. The first important observation is that the estimator reacts unusually slow, and only converges after multiple seconds (in contrast to the earlier hundreds of seconds). Secondly, notice how the measurements indicate the cart moves to the wrong direction, driving further from the wall as supposed to closer to the reference distance. The reason for this is obvious: At first, the estimated state was guessed at 10 cm, which is closer to the wall than the reference, thus sending a control signal sending the cart further backwards. After about a second, the estimate passes 15 cm, thus sending the cart in the right direction. This control performance is obviously less than satisfactory. The problem is pretty clear: the estimator reacts way too slow, which leads to wrong estimations and therefore ruining the control performance. This is very comparable to a Kalman filter that has a really low  $\frac{Q}{R}$  ratio and is thus overconfident in its state model. Note that, due to what is known as the separation principle, the controller pole did not move with respect to all earlier experiments and is not influenced by the estimator pole. The poor control performance is thus only due to the fact that the estimator is not accurate. To actually design a working state estimator, the pole has to be chosen at least 2 to 6 times faster than the control pole, instead of 10 times slower. Doing so, the total system dynamics is mostly determined by the slower controller pole, instead of the estimator pole, which would greatly increase the controller performance.

## References

- [1] Pipeleers and Swevers. *Control Theory - handouts*. Aug. 2020.